Published in final edited form as:

Cancer Res. 2009 January 1; 69(1): 45–54. doi:10.1158/0008-5472.CAN-07-6330.

Impaired Bub1 Function *In vivo* Compromises Tension-Dependent Checkpoint Function Leading to Aneuploidy and Tumorigenesis

Mark Schliekelman[1,2], **Dale O. Cowley**[2], **Ryan O'Quinn**[3], **Trudy G. Oliver**[2], **Lucy Lu**[2], **E.D. Salmon**[3], and **Terry Van Dyke**[2]

[1]Curriculum in Genetics, University of North Carolina at Chapel Hill, Chapel Hill, North Carolina

[2]Department of Genetics and the Lineberger Comprehensive Cancer Center, University of North Carolina at Chapel Hill, Chapel Hill, North Carolina

[3]Department of Biology, University of North Carolina at Chapel Hill, Chapel Hill, North Carolina

Abstract

Bub1 is a serine/threonine kinase originally described as a core component of the spindle assembly checkpoint (SAC) mechanism in yeast. Bub1 binding at kinetochores has been reported to be required for SAC function and localization of other SAC components. A proper SAC is believed to be essential for murine embryonic development, as all previously described null mutations in SAC components in mice cause embryonic lethality. We produced mice harboring a *Bub1* mutant allele lacking exons 2 and 3, resulting in a hypomorphic mutant expressed at <5% of wild-type levels. Despite this significant reduction, homozygous mutant animals are viable on a mixed 129P2/B6 or FVB background but display increased tumorigenesis with aging, whereas mice with a C57Bl/6J background die perinatally. Bub1 mutant murine embryonic fibroblasts (MEFs) display defects in chromosome congression to the metaphase plate, severe chromosome missegregation, and aneuploidy accompanied by high levels of premature senescence. Mutant MEFs have a robust SAC in response to nocodazole treatment but an impaired response to Taxol. Mutant MEFs also show reduced kinetochore localization of BubR1, but not of Mad2. The significant reduction in SAC response to Taxol, but not nocodazole, coupled with the reduced binding of BubR1, but not Mad2, indicates that Bub1 is particularly critical for the SAC response to a lack of tension on kinetochores. Thus, Bub1 is essential for proper chromosome segregation, a defect that can lead to severe phenotypes, including perinatal lethality and a predisposition to cancer.

Requests for reprints: Terry Van Dyke, University of North Carolina, 102 Mason Farm Road, CB 7295, Chapel Hill, NC 27514. Phone: 919-962-2145; Fax: 919-843-3160; tvdlab@med.unc.edu.
M. Schliekelman and D.O. Cowley contributed equally to this work.
Current address for D.O. Cowley: GlaxoSmithKline, Research Triangle Park, NC 27709. Current address for T.G. Oliver: Center for Cancer Research, Massachusetts Institute of Technology, Cambridge, MA 02142.

Note: Supplementary data for this article are available at Cancer Research Online (http://cancerres.aacrjournals.org/).

Disclosure of Potential Conflicts of Interest: No potential conflicts of interest were disclosed.

Introduction

Proper chromosome segregation is critical at every cell division to prevent aneuploidy, a condition associated with aggressive cancer, birth defects, and infertility (reviewed in ref. 1). The spindle assembly checkpoint (SAC) is a major guardian of mitotic fidelity. The SAC works as a checkpoint and timing mechanism to delay sister chromatid separation and anaphase onset until all chromosomes achieve bipolar attachment to microtubules at the metaphase plate. The SAC can be activated by lack of kinetochore-microtubule attachment or loss of tension on the kinetochore microtubules, thus allowing it to respond to the major types of aneuploidy-generating defects that arise during mitotic progression (reviewed in refs. 1–3). The SAC blocks anaphase entry by inhibiting the APC/Cdc20 complex, a multisubunit ubiquitin ligase that induces anaphase by promoting proteosomal degradation of mitotic substrates. The mechanism of APC/Cdc20 inhibition by the SAC is multitiered, including inhibitory binding of SAC components Mad2 and/or BubR1 to Cdc20 and Bub1-mediated inhibitory phosphorylation of APC/Cdc20 (3). Distinct inhibitory pathways may be activated by different conditions (e.g., loss of microtubule attachment versus loss of tension), although it remains unclear whether the different regulatory mechanisms function in separate pathways or as part of an integrated signaling system. The relative contributions of each mechanism to overall mitotic fidelity are also not well understood.

The spindle checkpoint machinery is encoded by a core group of genes originally identified in *Saccharomyces cerevisiae*, including *Mad1–3*, *Bub1*, *Bub3*, and *Mps1*. Yeasts lacking core SAC components grow normally under unperturbed conditions yet display increased rates of chromosome missegregation and are unable to grow in the presence of spindle poisons, such as nocodazole (4–6). Studies of SAC function in mammals have been limited by the fact that murine null mutations in core SAC components, including *Bub3*, *Mad1*, *Mad2*, and *BubR1*, cause very early embryonic lethality, precluding analysis of embryonic fibroblasts or later developmental stages in null mutants (7–10). However, mouse embryonic fibroblasts (MEF) heterozygous for Mad2, Bub3, and BubR1 displayed haploinsufficiency, resulting in higher levels of mitotic abnormalities (9, 11, 12). Furthermore, whereas heterozygous animals were viable in each case, they displayed increased age-related spontaneous (11) or carcinogen-induced (9, 13) tumorigenesis. Mice with a hypomorphic *BubR1* allele that reduced BubR1 levels to ∼11% of wild type (wt) were viable but displayed cellular senescence, growth retardation, and progeroid features without a significant increase in tumor formation (12). These studies indicate that the SAC is essential for early embryonic development in mammals but that the phenotypes obtained from incomplete SAC impairment may vary across a broad range, depending on the depleted component and the degree of depletion. SAC components may also have SAC-independent functions that contribute to the observed phenotypes in some cases (14–16).

Despite its identification as a core spindle checkpoint component in yeasts, the functions of Bub1 have not been fully elucidated. Bub1 is a serine/threonine kinase that localizes to kinetochores during mitosis and mediates efficient kinetochore localization of other SAC components. Bub1 deletion in yeasts causes high chromosome missegregation rates under normal growth conditions, in addition to lethality under perturbed conditions (4–6). Studies in vertebrate systems have been confined to biochemical and cell culture models and have

produced some conflicting results about Bub1 roles in mitotic regulation. Bub1 is essential for spindle checkpoint activity in *Xenopus* extracts, and the bulk of this activity requires the NH_2 terminus, with minor requirements for the COOH terminal kinase functions (17, 18). In cultured mammalian cell lines, Bub1 reduction via RNA interference (RNAi) produced conflicting results. In one case, Bub1 was surprisingly dispensable for the SAC function but was required for chromosome congression (15). An independent study found that Bub1 was required for a functional SAC response to nocodazole while confirming the role in chromosome congression (16). These differences are difficult to reconcile but may stem from distinct levels of Bub1 depletion and/or differences in cell lines used for the studies. More recent studies have revealed a role for Bub1 in meiotic and mitotic sister chromatid cohesion via interaction with shugoshin (19, 20). Finally, compromised Bub1 function has been indirectly associated with tumorigenesis, indicating an important need to understand the molecular links associated with Bub1 function, mitotic regulation, and tumor suppression (21–24).

To better understand Bub1 functions and the consequences of Bub1 loss *in vivo*, we developed a conditional *Bub1* mutation in mice. We report here that this mutation is hypomorphic, causing a severe reduction in Bub1 levels. Mice homozygous for the *Bub1* hypomorph mutation are viable on mixed 129P2/B6 and FVB genetic backgrounds but display high rates of tumorigenesis. The mutant phenotype is more severe on a C57Bl/6J background, where homozygous mutants die perinatally. In MEFs, *Bub1* mutation causes high rates of chromosome missegregation and aneuploidy, accompanied by growth defects and premature senescence. Surprisingly, the spindle checkpoint is functional in *Bub1* mutant MEFs, although the checkpoint response to Taxol is significantly impaired. BubR1 kinetochore localization is markedly reduced in *Bub1* mutant MEFs, consistent with the conclusion that Bub1 plays a key role in a BubR1-dependent tension-sensitive SAC response. These findings indicate that Bub1 is critical for proper progression through mitosis and that defects in Bub1 signaling cause severe defects ranging from early lethality to tumorigenesis.

Materials and Methods

Bub1 gene targeting and mice

Bub1 genomic BAC clones were isolated from a 129SvEv library by hybridization screening and subsequent PCR verification. The bacterial strain EL350 (25) was used for “recombineering” to subclone a 13-kb fragment encompassing *Bub1* exons 1 to 6 into a pUC19-based plasmid, including a phosphoglycerate kinase–thymidine kinase gene (a gift of R. Thresher, University of North Carolina Animal Models Core Facility). A loxP site was inserted in intron 1 by recombineering a loxP-flanked zeocin cassette, followed by Cre-mediated cassette removal in EL350. A loxP and FRT-flanked neomycin resistance cassette was subsequently inserted into intron 3. The targeting vector was linearized and used for gene targeting in E14 ES cells (129P2/OlaHsd strain). ES cell targeting was verified by PCR and Southern blot, and correctly targeted clones were injected into C57Bl/6J blastocysts for chimera generation. Chimeric males were bred to C57Bl/6J females, and germline transmission of the $Bub1^{neo}$ allele was verified by PCR. The $Bub^{\Delta 2\text{-}3}$ and $Bub1^{f}$ alleles were

generated by crossing the *Bub1*^{neo} allele with an X-linked CMV-Cre strain (26). *Bub*$^{\Delta 2\text{-}3}$ viability phenotypes were studied on three genetic backgrounds: 129/B6 (F2-F4), B6N4+, and FVBN7+. For the FVB studies, the *Bub1*$^{\Delta 2\text{-}3}$ allele was independently derived from the *Bub1*^{neo} allele by crossing (FVBN5)*Bub1*$^{neo/+}$ animals to an FVB-β-actin-Cre deleter strain. The Cre transgene was removed by segregation before intercrossing *Bub*$^{\Delta 2\text{-}3/+}$ animals. MEF studies were performed with MEFs derived from embryos on the C57Bl/6J background (B6N4+). All mice were maintained according to the Institutional Animal Care and Use Committee at the University of North Carolina at Chapel Hill.

Bub1^{GT8} allele

Bub1 gene-trapped ES cell clone XG453 was obtained from Bay Genomics. The gene trap is produced by a splice-acceptor-β-geo cassette within *Bub1* intron 7. XG453 ES cells were injected into C57Bl/6J blastocysts, and resulting chimeras were bred to C57Bl/6J females and screened for germline transmission by PCR. Animals used in experiments reported here were backcrossed one to two generations to C57Bl/6J. All animal experiments were approved by the Institutional Animal Care and Use Committee of the University of North Carolina at Chapel Hill.

Cell culture

MEF lines were generated from e13.5-e14.5 using standard protocols. MEFs were cultured at 5% CO_2 in media containing DMEM-H with 10% fetal bovine serum, 2 mmol/L glutamine, 50 μg/mL penicillin, 50 μg/mL streptomycin, and 55 μmol/L 2-mercaptoethanol and were passaged every 2 d by plating 500,000 viable cells. All experiments with MEFs were performed at passages 3 to 4, unless otherwise stated. Growth curves were generated by counting total number of viable cells at each passage. Drug treatments were used at the following concentrations: nocodazole (Sigma-Aldrich), 200 ng/mL; paclitaxel (Sigma-Aldrich), 1 μmol/L; MG132 (Calbiochem), 10 μmol/L.

Spindle checkpoint analysis

Asynchronously growing MEFs were treated with 200 ng/mL nocodazole for indicated times, trypsinized, fixed for 20 min in 1% formaldehyde, spun down, and resuspended in 70% cold ethanol. For flow cytometry, cells were stained with anti–phosphorylated histone H3 (Upstate Biotechnology) at 1:500 and Alexafluor 488 (Invitrogen) at 1:1,000, followed by propidium iodide. Cells (30,000) were analyzed on a Becton Dickinson FACScan, and the number of phosphorylated histone H3– postive cells was measured as a percentage of total cells.

Immunofluorescence

Coverslips were fixed in 2% formaldehyde, permeablized in PBS + 0.5% Triton X-100 (PBS-TX), and washed in PBS. After blocking for 30 min in PBS-TX plus 5% nonfat dried milk (NFDM) or bovine serum albumin (BSA), coverslips were incubated overnight with primary antibodies. Antibodies were used at the following concentrations: rabbit anti–phosphorylated histone H3,1:500 (Upstate Biotechnology); anti–β-tubulin, 1:250 (Tub2.1, Sigma-Aldrich); sheep anti-Bub1, 1:500 (Steve Taylor); rabbit anti-Mad2, 1:500 (E.D.

Salmon); rabbit anti-BubR1, 1:500 (BD Biosciences); human anti-centromere, 1:500 (ACA, Antibodies Incorporated.). After washes with PBS-TX, coverslips were incubated for 1 h with appropriate secondary antibodies (Alexafluor 488 or 594) at 1:500 in PBS-TX plus 5% NFDM or BSA, washed with PBS-TX, stained with 4′,6-diamidino-2-phenylindole (DAPI), and mounted with Flouromount G (Electron Microscopy Sciences). Analysis was carried out on a Leica DMRXA microscope. See supplementary data for specifics on kinetochore localization methods.

Karyotyping

MEFs at passage 5 were treated with Karyomax colcemid (Invitrogen) for 4 h, trypsinized, resuspended in warm 75 mmol/L hypotonic KCl buffer, and incubated for 20 min. Cells were washed at least four times in Carnoy's buffer before being resuspended in fresh Carnoy's fix, dropped into cold, ethanol-washed slides, and stained with DAPI. Images of single-cell spreads were acquired on a Leica DMRXA microscope with a 63 × objective. Chromosomes from distinct individual cells were counted, with chromosome numbers of >70 for a sinsgle cell being discarded as endoreduplication.

Senescence assay

MEFs grown on coverslips at indicated passages were fixed in 1% formaldeyde and 0.1% glutaraldehyde for 5 min before being treated overnight (14–18 h) in senescence-associated β-galactosidase assay buffer (see ref. 27). Cells were counterstained with DAPI, and cells, staining positive for senescence, were counted as a percentage of total cells.

Western blotting and immunoprecipitation

Subconfluent MEFs were treated with 200 ng/mL nocodazole for 6 h, lysed in modified radioimmunoprecipitation assay buffer, separated by SDS-PAGE, and transferred to nitrocellulose membranes. Membranes were blocked for 30 to 60 min in PBS + 0.1% Tween 20 (PBS-T) with 5% NFDM, incubated overnight at 4°C with anti-Bub1 at 1:1,000 (a kind gift from Steve Taylor), and diluted in PBS-T + 5% NFDM. For immunoprecipitation, plates of subconfluent cells were treated with 200 ng/mL of nocodazole for 6 h and 10 μm of MG132 for 2 h. Cells were collected from plates as above. Total protein (500 μg) was incubated overnight at 4°C with 50 μL anti-Bub1 sera (28).

Results

Generation of the *Bub1*$^{\Delta 2\text{-}3}$ allele

We generated a conditional mutation of the murine Bub1 gene by homologous recombination in ES cells. Based on available sequence information, deletion of exons 2 and 3 was predicted to cause a null allele by creating a frameshift early in exon 4, leading to a premature stop codon in exon 6 (Fig. 1A). The targeting construct was designed with a loxP site in intron 1 and a loxP-flanked neomycin resistance cassette in intron 3, thus allowing deletion of exons 2 and 3 by Cre-mediated recombination (Supplementary Fig. S1A). Correctly targeted ES cell clones were used to generate chimeric founders that transmitted the *Bub1*^{neo} allele through the germline (Supplementary Fig. S1B). *Bub1*$^{neo/+}$ mice were crossed to a germline Cre deleter strain (see Materials and Methods) to produce the *Bub1*

floxed allele (*Bub1*^{f}) by removal of the neomycin resistance cassette and the *Bub1*$^{\Delta 2\text{-}3}$ allele by removal of the neo cassette and exons 2 and 3. *Bub1*$^{neo/+}$, *Bub1*$^{f/+}$, and *Bub1*$^{\Delta 2\text{-}3/+}$ mice are viable and fertile. Genotypes were confirmed by PCR (Supplementary Fig. S1C).

Bub1$^{\Delta 2\text{-}3/\Delta 2\text{-}3}$ survival is dependent on genetic background

Homozygous deletion of spindle checkpoint genes *Mad2*, *Bub3*, and *BubR1* in mice causes embryonic lethality at e4.5-7.5 during rapid expansion of the inner cell mass (7, 8, 10). *Bub1*$^{\Delta 2\text{-}3/+}$ mice were intercrossed to test whether Bub1 loss also causes early embryonic lethality. Surprisingly, *Bub1*$^{\Delta 2\text{-}3/\Delta 2\text{-}3}$ animals were obtained at near Mendelian ratios from intercrosses on a mixed 129P2/B6 genetic background (Table 1). However, intercrosses performed after backcrossing four or more generations to C57Bl/6J yielded live *Bub1*$^{\Delta 2\text{-}3/\Delta 2\text{-}3}$ animals at only 20% of expected Mendelian frequency (Table 1), and nearly all live-born (B6)*Bub1*$^{\Delta 2\text{-}3/\Delta 2\text{-}3}$ mice died perinatally. (B6)*Bub1*$^{\Delta 2\text{-}3/\Delta 2\text{-}3}$ mice seemed to breathe and nurse normally but displayed runting and failure to thrive in the early postnatal period. The average weight of *Bub1*$^{\Delta 2\text{-}3/\Delta 2\text{-}3}$ animals was 1.19 ± 0.06 g versus 1.41 ± 0.13 g for wt ($P < 0.01$) on day of birth. To date, only two homozygous animals survived to weaning at 21 days. To determine when the remaining 80% of (B6)*Bub1*$^{\Delta 2\text{-}3/\Delta 2\text{-}3}$ mice die, embryos were generated from (B6)*Bub1*$^{\Delta 2\text{-}3/+}$ intercrosses at E13.5-14.5 and E17.5-18.5. At both E13.5-14.5 and E17.5-18.5, (B6)*Bub1*$^{\Delta 2\text{-}3/\Delta 2\text{-}3}$, (B6)*Bub1*$^{\Delta 2\text{-}3/+}$, and (B6)*Bub1*$^{+/+}$ embryos were recovered at Mendelian ratios (Table 1). Histologic analysis of sections from e14.5 and e18.5 whole embryos did not reveal any morphologic defects (data not shown). Observations of cell death in the liver and the marked paleness of some (B6)*Bub1*$^{\Delta 2\text{-}3/\Delta 2\text{-}3}$ embryos led us to perform cell blood count analysis on blood from e18.5 embryos, revealing mild anemia and leukocytosis. In summary, (B6)*Bub1*$^{\Delta 2\text{-}3/\Delta 2\text{-}3}$ mice displayed perinatal lethality of unknown cause, whereas *Bub1*$^{\Delta 2\text{-}3/\Delta 2\text{-}3}$ animals were viable on a 129/B6 mixed background. We also derived the *Bub1*$^{\Delta 2\text{-}3}$ allele on an FVB genetic background, in which (FVB)*Bub1*$^{\Delta 2\text{-}3/\Delta 2\text{-}3}$ animals are obtained at Mendelian ratios (Table 1). Together, these results indicate that that the phenotype of the *Bub1*$^{\Delta 2\text{-}3}$ allele is modified by the genetic background. The perinatal lethal phenotype of (B6)*Bub1*$^{\Delta 2\text{-}3/\Delta 2\text{-}3}$ animals is similar to that of mice harboring a hypomorphic mutation of the BubR1 spindle checkpoint gene (12), as well as mice with mutations of DNA damage genes, such as BRCA2 (29). This observation, coupled with results from inactivation of other spindle checkpoint genes in mice, strongly suggests that the Bub1$^{\Delta 2\text{-}3}$ allele retains partial function.

The *Bub1*$^{\Delta 2\text{-}3}$ allele is hypomorphic

The recovery of viable *Bub1*$^{\Delta 2\text{-}3/\Delta 2\text{-}3}$ mice suggested the *Bub1*$^{\Delta 2\text{-}3}$ allele may be hypomorphic rather than null. To test this hypothesis, we obtained mice harboring a *Bub1* gene-trap allele with a β-geo cassette and splice acceptor inserted in intron 7 (see Materials and Methods). Intercrosses of *Bub1*$^{gt8/+}$ animals revealed a likely maternal defect in breeding, as very few live mice of any genotype were recovered from these crosses and 90% of embryos were resorbed by e14.5. Crosses of *Bub1*$^{\Delta 2\text{-}3/+}$ females with *Bub1*$^{gt8/+}$ males showed that compound heterozygous (*Bub1*$^{\Delta 2\text{-}3/gt8}$) animals were absent before e11.5 (Table 1). Because the genetic background in these experiments is mixed 129/B6 (a background that supported survival of *Bub1*$^{\Delta 2\text{-}3/\Delta 2\text{-}3}$ animals), the failure to recover compound

heterozygous animals at midgestation is strong genetic evidence that the *Bub*$^{\Delta 2\text{-}3}$ allele is hypomorphic, as the *Bub1*^{gt8} allele is apparently more severe.

To determine the nature of the *Bub1*$^{\Delta 2\text{-}3}$ mutation, we first analyzed mRNA production in MEFs from E14.5 embryos. Quantitative reverse transcription–PCR (RT-PCR; not shown) and Northern hybridization analysis showed equivalent RNA levels in *Bub1*$^{+/+}$ and *Bub1*$^{\Delta 2\text{-}3/\Delta 2\text{-}3}$ MEFs (Supplementary Fig. S2A). *Bub1*$^{\Delta 2\text{-}3/\Delta 2\text{-}3}$ MEFs expressed a single Bub1 mRNA that was smaller than the wt mRNA, consistent with the deletion of exons 2 and 3. cDNA from *Bub1*$^{\Delta 2\text{-}3/\Delta 2\text{-}3}$ MEFs was cloned and sequenced, demonstrating that the mRNA produced from the mutant allele is spliced from exon 1 to exon 4, as predicted (Supplementary Fig. S2B). No novel alternatively spliced RNAs were detected by Northern or RT-PCR analyses using various primer sets across the Bub1 mRNA sequence (data not shown). Together, these data suggest that the residual function of the *Bub1*$^{\Delta 2\text{-}3}$ allele, if any, must be derived from the Δ2-3 mutant mRNA.

Analysis of the predicted mRNA from the *Bub1*$^{\Delta 2\text{-}3}$ allele suggested two alternative possibilities for mutant protein expression: (*a*) an ATG codon 5′ to the published start codon could produce a protein that is out of frame until reaching the exon 1 to exon 4 splice but in-frame thereafter (aa77–aa1058) and/or (*b*) translation from in-frame internal ATGs present in exon 4 or beyond producing NH_2 terminal truncations (aa103 or aa173–aa1058; Fig. 1A). These ATGs are not in Kozak consensus sequences but could still give rise to protein (30). To distinguish these possibilities, we analyzed protein from *Bub1*$^{\Delta 2\text{-}3/\Delta 2\text{-}3}$ MEFs by Western blot using an antibody raised against Bub1 aa336-aa489 (31). No Bub1 protein was detected in extracts from *Bub1*$^{\Delta 2\text{-}3/\Delta 2\text{-}3}$ MEFs, whereas *Bub1*$^{\Delta 2\text{-}3/+}$ and *Bub1*$^{+/+}$ MEFs expressed a Bub1 protein of expected size (Fig. 1B). Likewise, no protein was detected in 129/Bl6 *Bub1*$^{\Delta 2\text{-}3/\Delta 2\text{-}3}$ MEFs or tissues (data not shown). Titration of wt cell lysate showed the sensitivity of Bub1 detection to be 5% of normal endogenous levels (Fig. 1C), indicating that the *Bub1*$^{\Delta 2\text{-}3}$ allele disrupts production of the wt Bub1 protein and that any protein produced from the mutant allele must be produced at <5% of wt levels. Immunoprecipitation–Western blot analysis using an antibody recognizing residues 1-331 of the Bub1 protein for immunoprecipitation (28) and the antibody recognizing residues 336-489 for Western blot analysis (31) detected a mutant-specific band of ∼115 kDa in *Bub1*$^{\Delta\Delta 2\text{-}3/\Delta 2\text{-}3}$ and *Bub1*$^{\Delta 2\text{-}3/+}$ samples (Fig. 1D). This protein could be produced by translation from either an upstream or downstream ATG and, thus, lacks at least the NH_2 terminal 73 aa of Bub1. Thus, the phenotypes observed in *Bub1*$^{\Delta 2\text{-}3/\Delta 2\text{-}3}$ mice and MEFs could be due to the lack of a critical NH_2 terminal Bub1 domain, severely diminished protein levels, or both.

Bub1 and BubR1 kinetochore localization are reduced in *Bub1*$^{\Delta 2\text{-}3/\Delta 2\text{-}3}$ MEFs

Bub1 localizes to kinetochores in response to lack of spindle attachment and/or tension and is required for efficient localization of other spindle checkpoint proteins that mediate the spindle checkpoint activity (15). The domain required for Bub1 kinetochore localization is encoded by exon 8 and is, thus, likely to be included in the protein encoded by the *Bub1*$^{\Delta 2\text{-}3}$ allele (32). Nevertheless, Bub1 staining at kinetochores of *Bub1*$^{\Delta 2\text{-}3/\Delta 2\text{-}3}$ MEFs was only 2% of wt (Fig. 2A), consistent with severely reduced total levels of mutant Bub1 protein.

In cultured cell lines, Bub1 is required for efficient kinetochore localization of other spindle checkpoint proteins, such as Mad2 and BubR1 in response to SAC activation (15, 33). SAC activation can be modeled experimentally by treating cells with nocodazole (which causes a loss of kinetochore-spindle attachment and tension) or Taxol (which disrupts tension forces between kinetochores while leaving attachments intact). Using immunofluorescence, we examined the Mad2 and BubR1 at kinetochores of $Bub1^{\Delta 2\text{-}3/\Delta 2\text{-}3}$ MEFs after nocodazole or Taxol treatment. However, significant cell-to-cell variation and high background with ACA staining precluded accurate measurement (Supplementary Fig. S3). To control for the variance, cells singly stained with Mad2 or BubR1 were counted and classified according to level of kinetochore localization (Fig. 2B): ++++, bright kinetochore staining; +++, dim above background kinetochore staining; ++, kinetochore staining at punctate background levels; +, no kinetochore staining. Using this stratification, a clear difference in kinetochore localization of BubR1, but not Mad2, was detected in response to both nocodazole and Taxol. Mad2 staining was clearly evident at kinetochores (++++ or +++) in 100% of $Bub1^{+/+}$ and 93% of $Bub1^{\Delta 2\text{-}3/\Delta 2\text{-}3}$ MEFs after nocodazole treatment. Mad2 localization after Taxol treatment is comparably weak in both wt and mutant cells (Fig. 2C). In contrast, BubR1 kinetochore localization was greatly reduced in $Bub1^{\Delta 2\text{-}3/\Delta 2\text{-}3}$ cells when treated with nocodazole (44% of cells had clear kinetochore localization versus 99% of wt; $P < 0.05$) or Taxol (15% versus 83%, respectively, $P < 0.05$; Fig. 2D). These results indicate that Bub1 is necessary for proper BubR1 kinetochore localization in response to lack of kinetochore-microtubule attachment and, particularly, to the lack of microtubule tension.

$Bub1^{\Delta 2\text{-}3/\Delta 2\text{-}3}$ MEFs exhibit a defective spindle checkpoint, chromosome segregation errors, and increased aneuploidy

Kinetochore localization of SAC proteins Mad2 and BubR1 has previously been speculated to be necessary for SAC function. The reduced BubR1 kinetochore localization in $Bub1^{\Delta 2\text{-}3/\Delta 2\text{-}3}$ MEFs suggested that these cells may have a defective SAC response. We tested spindle checkpoint responses of $Bub1^{\Delta 2\text{-}3/\Delta 2\text{-}3}$, $Bub1^{\Delta 2\text{-}3/+}$, and wt MEFs by measuring mitotic indices (percentage of positive phosphorylated histone H3) after treatment with nocodazole or Taxol. $Bub1^{+/+}$, $Bub1^{\Delta 2\text{-}3/+}$, and $Bub1^{\Delta 2\text{-}3/\Delta 2\text{-}3}$ MEFs all showed an increased mitotic index by 12 hours after nocodazole addition compared with untreated cultures, indicating that each genotype retains at least partial SAC function in response to spindle ablation (Fig. 3A). Nocodazole-treated $Bub1^{\Delta 2\text{-}3/+}$ and $Bub1^{\Delta 2\text{-}3/\Delta 2\text{-}3}$ cultures contained only modestly lower indices (5.8% and 7%, respectively) than the $Bub1^{+/+}$ cultures (8.9%). This result contrasts with reported results from MEFs heterozygous for a null mutation in Bub3 or a hypomorphic mutation of BubR1, which show a severely impaired arrest in response to nocodazole treatment (9, 12). Likewise, there was no increase in premature sister chromatid separation after treatment with colcemid (2.5% in $Bub1^{\Delta 2\text{-}3/\Delta 2\text{-}3}$ versus 1.5% in $Bub1^{+/+}$), another microtubule depolymerizing agent. In contrast to nocodazole treatment, $Bub1^{\Delta 2\text{-}3/\Delta 2\text{-}3}$ MEFs did display a severe SAC defect in response to Taxol treatment (mitotic index, 3.5% for $Bub1^{\Delta 2\text{-}3/\Delta 2\text{-}3}$ versus 8% for $Bub1^{+/+}$; Fig. 3A). These data suggest that reduced protein levels and/or NH_2 terminal deletion of Bub1 is more detrimental to the response to the loss of tension than the loss of attachment.

The primary role of the spindle checkpoint is to aid proper segregation of the chromosomes by delaying anaphase until all chromosomes are attached and under tension by spindle fibers. Loss of the spindle checkpoint has been linked to increased aneuploidy in several models of spindle checkpoint loss (9, 12). To test whether relaxation, but not complete abrogation of the spindle checkpoint, can increase aneuploidy under normal growth conditions, we determined the chromosome counts in metaphase spreads from Bub1 mutant and wt MEFs. Seventy-six percent of metaphases from *Bub1*$^{\Delta 2\text{-}3/\Delta 2\text{-}3}$ MEFs were aneuploid, compared with 9% of *wt* and 23% of *Bub1*$^{\Delta 2\text{-}3/+}$ metaphases (Fig. 3B). Most of the aneuploid cells showed gain or loss of only one to two chromosomes. These high levels of aneuploidy represent an extreme level of chromosome instability, indicating that Bub1 is essential for proper chromosome segregation under unperturbed growth conditions.

Whereas the aneuploidy in *Bub1*$^{\Delta 2\text{-}3/\Delta 2\text{-}3}$ MEFs could be due to a relaxed spindle checkpoint, Bub1 has also been implicated in proper chromosome congression (i.e., the movement of chromosomes to the metaphase plate; refs. 15, 16). To test whether *Bub1* mutant MEFs congress chromosomes properly, synchronized MEFs were treated with the proteasome inhibitor MG132 as cells were entering mitosis. Inhibiting the proteasome blocks securin and cyclin B degradation, preventing the separation of sister chromatids at the metaphase plate and stopping mitosis in metaphase. Defects in chromosome congression are detected by an increase in chromosomes that have not aligned at the metaphase plate. Consistent with previous RNAi studies (15, 16), MG132-treated *Bub1*$^{\Delta 2\text{-}3/\Delta 2\text{-}3}$ MEFs showed an increase in chromosome congression defects, with 19.6% of mutant versus 5.7% of *wt* MEFs displaying uncongressed chromsomes (Fig. 3C). This result supports the conclusion that Bub1 plays a role in chromosome congression and suggests that defective congression may contribute to extreme aneuploidy of *Bub1*$^{\Delta 2\text{-}3/\Delta 2\text{-}3}$ MEFs.

Uncongressed chromosomes should trigger a SAC response, delaying anaphase onset until congression is complete and kinetochores are under tension. We reasoned that the reduced sensitivity of the SAC response in *Bub1*$^{\Delta 2\text{-}3/\Delta 2\text{-}3}$ MEFs may allow cells to enter anaphase despite the presence of one or more unattached or mono-oriented kinetochores, resulting in daughter cells with gain or loss of one to two chromosomes. This model predicts that unperturbed cells should have high rates of anaphase lagging chromosomes. Indeed, analysis of unperturbed *Bub1*$^{\Delta 2\text{-}3/\Delta 2\text{-}3}$ MEFs during anaphase revealed that 47% of *Bub1*$^{\Delta 2\text{-}3/\Delta 2\text{-}3}$ MEFs in anaphase had one or more lagging chromosomes compared with only 9% of wt and 8% of heterozygotes (Fig. 3D). Taken together, these results suggest that the extreme aneuploidy of *Bub1*$^{\Delta 2\text{-}3/\Delta 2\text{-}3}$ MEFs is caused by a combination of defects in chromosome congression and SAC activation.

Bub1$^{\Delta 2\text{-}3/\Delta 2\text{-}3}$ MEFs are growth impaired with high rates of senescence

High levels of aneuploidy in BubR1 hypomorphic animals and MEFs correlated with growth impairment and high levels of senescence (12). Furthermore, a recent study indicated that RNAi knockdown of Bub1 in primary human fibroblasts resulted in increased senescence (34). We determined growth and senescence rates in Bub1$^{\Delta 2\text{-}3/\Delta 2\text{-}3}$ MEFs to assess whether similar phenotypes occur in this system. Wt and heterozygous cultures grew at similar rates, with expected decreases in cell accumulation at higher passages due to senescence (35),

whereas *Bub1*$^{\Delta 2\text{-}3/\Delta 2\text{-}3}$ MEFs grew much more slowly (Fig. 4A). To ascertain the cause of the growth differences, we assessed levels of apoptosis and senescence. *Bub1*$^{\Delta 2\text{-}3/\Delta 2\text{-}3}$ MEFs did not show increased apoptosis relative to wt and heterozygous cells, as measured by Annexin V staining (data not shown). However, senescence-associated β-galactosidase assays revealed that *Bub1*$^{\Delta 2\text{-}3/\Delta 2\text{-}3}$ MEFs had a significant increase in senescence compared with *wt* MEFs at passage 3 (9.1% versus 3.1) and passage 5 (15.4% versus 4.4%) examined (Fig. 4B and C). The percentage of BrdUrd incorporating cells was also lower in *Bub1*$^{\Delta 2\text{-}3/\Delta 2\text{-}3}$ MEFs, consistent with the increase in senescent cells (not shown). *Bub1*$^{\Delta 2\text{-}3/\Delta 2\text{-}3}$ MEFs did not show marked increases in the DNA damage marker phosphorylated H2AX (3.1% versus 2.6% in *wt* MEFs; Fig. 4D), indicating that DNA breaks did not contribute significantly to the senescent phenotype. These results indicate that the high levels of chromosome missegregation and aneuploidy in *Bub1*$^{\Delta 2\text{-}3/\Delta 2\text{-}3}$ cells trigger growth impairment via premature senescence.

Impaired Bub1 function predisposes to increased tumorigenesis

Aneuploidy arising from spindle checkpoint impairment or other defects has long been hypothesized to contribute to tumor formation. In support of this hypothesis, most heterozygous mouse spindle checkpoint mutants generated to date have shown modest increases in spontaneous and/or carcinogen-induced tumor formation (11–13, 36). However, some evidence suggests that extreme aneuploidy may inhibit tumorigenesis (12, 37). To determine if Bub1 impairment contributes to tumor formation, cohorts of (129/B6)*Bub1*$^{\Delta 2\text{-}3/\Delta 2\text{-}3}$ and controls were of ages of 2 years. Approximately, 76% of (129/B6)*Bub1*$^{\Delta 2\text{-}3/\Delta 2\text{-}3}$ mice developed tumors by 23 to 25 months compared with 42% of (129/B6)*Bub1*$^{\Delta 2\text{-}3/+}$ ($P < 0.05$) and ∼28% of (129/B6)*Bub1*$^{+/+}$ animals ($P < 0.05$; Fig. 5A) As in aging *wt* mice, the majority of (129/B6)*Bub1*$^{\Delta 2\text{-}3/\Delta 2\text{-}3}$ tumors were of liver origin and occurred at an increased frequency. Importantly, *Bub1* mutation also broadened the tumor spectrum. Lung tumors appeared in 16% (4 of 25) of (129/B6)*Bub1*$^{\Delta 2\text{-}3/\Delta 2\text{-}3}$ mice, whereas no lung tumors were found in *wt* littermate controls (Fig. 5B). Whereas a significant increase in spontaneous tumors was not observed in the (129/B6)*Bub1*$^{\Delta 2\text{-}3/+}$ cohort, a lung tumor and a brain tumor were observed, suggesting a possible change in tumor spectrum. These data indicate that Bub1 is a low penetrance tumor suppressor, likely with significant quantitative effects based on the genetic modification of phenotypes in distinct genetic backgrounds. Together with the results from *Bub1*$^{\Delta 2\text{-}3/\Delta 2\text{-}3}$ MEFs, these data indicate that chromosome missegregation defects leading to aneuploidy in cells of *Bub1* mutant mice drive postnatal developmental defects ranging from lethality to tumor formation, depending on the associated genetic context.

Discussion

We have probed the functions of the mammalian mitotic regulator Bub1 by generating a hypomorphic mutation (*Bub1*$^{\Delta 2\text{-}3}$) in mice that lacks part of an NH_2 terminal conserved domain implicated in spindle checkpoint function in yeast. In addition, the protein is expressed at severely diminished levels, yet retains sufficient function to support development to birth or adulthood, depending on genetic context. In the C57Bl6/J background, homozygous mutant mice die perinatally with a “failure-to-thrive” phenotype,

whereas FVB and mixed 129P2/C57Bl6/J backgrounds support survival to late adulthood. However, these mice develop a high incidence of cancers compared with wt littermates solidifying a role for impaired Bub1 function in tumorigenesis.

Bub1$^{\Delta 2\text{-}3}$ was characterized as a hypomorphic mutant by demonstrating that compound heterozygotes with a gene-trapped allele, *Bub1*^{gt8}, die by E11.5. Indeed, two contemporary reports show that *Bub1 null* mutants arrest by E7.5 (38, 39), consistent with the early embryonic lethality previously described for homozygous null mutants of the SAC genes *Mad2*, *BubR1*, and *Bub3* (7, 8, 10). Based on the proposed *Bub1* ATG translation start site, the *Bub1*$^{\Delta 2\text{-}3}$ mutation was designed to produce a severely truncated protein lacking the kinase domain and expected to be nonfunctional. Analyses of the mRNA expressed in mutant MEFs indicate that the transcript lacking exons 2 and 3 is expressed at normal levels. Immunoprecipitation–Western blot analysis of nocodazole-arrested MEFs identified a unique protein in *Bub1*$^{\Delta 2\text{-}3/+}$ and *Bub1*$^{\Delta 2\text{-}3/\Delta 2\text{-}3}$ MEFs, which is ∼5 kDa smaller than *wt Bub1* and present at <5% of *wt* levels. Thus, the mutant Bub1 protein seems to be produced by translation from an alternative ATG, the most likely of which would give rise to an NH_2 terminal truncation starting at exon 4, which retains the COOH terminal kinase domain and the kinetochore binding domain. The NH_2 terminal domain of Bub1 is highly conserved in nearly all species, but its function is still largely unknown. In fission yeast, checkpoint activity and kinetochore localization were mapped to residues 28-160, whereas mammalian Bub1 residues 200-300 were found to be required for SAC function and kinetochore localization (6, 32). Because the mutant protein is expressed at such low levels, the current studies cannot distinguish whether impaired function results from deletion of a critical NH_2 terminal function, insufficient protein, or both. Future studies will help to distinguish these possibilities, as well as determine the reason for the background-dependent phenotypic differences found in C57Bl6/J and FVB or mixed background mice. Nonetheless, this mutant provides a tool for probing the effects of reduced Bub1 functions in cells and during embryonic and adult development.

Bub1 in mitotic checkpoint regulation

MEFs derived from mutant and wt littermate embryos were used to assess the cellular phenotypes associated with impaired Bub1 function. A recent RNAi study in cell lines questioned a role for mammalian Bub1 in SAC function (15), whereas a distinct study found that Bub1 depletion ablated the SAC (16). We show here that, despite undetectable levels of Bub1 binding at kinetochores, Mad2 is able to localize at kinetochores in *Bub1*$^{\Delta 2\text{-}3/\Delta 2\text{-}3}$ MEFs, which arrest in mitosis when treated with nocodazole. These surprising results indicate that very little Bub1 is required for SAC activity in response to microtubule ablation in MEFs. Perera and colleagues (39) recently found that *Bub1-null* MEFs do not show a sustained arrest after treatment with nocodazole, whereas Jeganathan and colleagues (38) showed that MEFs with ∼20% of *wt* Bub1 activity arrest for a shorter duration than *wt* MEFs in nocodazole. The distinct methodologies used (duration of mitotic arrest versus mitotic index) make it difficult to directly compare these results to ours and could be responsible for the discrepancy. However, this inconsistency raises the possibility of a scenario where we have underrepresented the amount of Bub1Δ2-3 protein expressed and are primarily observing the effects of the NH_2 terminal deletion of the allele. Nevertheless,

our results are supported by previous findings with Bub1 small interfering RNA that only 5% of endogenous levels could support a mitotic arrest with spindle ablation (15, 16). These results together are consistent with a model in which a small amount of Bub1 is sufficient to arrest cells in response to spindle ablation. This contrasts with the haploinsufficiency of the SAC function in MEFs heterozygous for *Bub3* or hypomorphic for *BubR1*, which show very little mitotic arrest after nocodazole treatment (9, 12).

In contrast to Mad2, BubR1 kinetochore localization is reduced in *Bub1*$^{\Delta 2\text{-}3/\Delta 2\text{-}3}$ MEFs in response to nocodazole and is further reduced after Taxol treatment. A similar reduction in BubR1 kinetochore localization was recently observed in *Bub1-null* and *hypomorph* MEFs, providing a strong consensus that Bub1 is critical for BubR1 localization (38, 39). Previous kinetochore localization studies suggest that BubR1 is responsive to changes in tension, whereas Mad2 binds kinetochores in response to attachment failure (40). The inhibition of APC/Cdc20 in response to nocodazole may be due to integration of signals from both pathways (as evidenced by strong localization of both BubR1 and Mad2 with nocodazole treatment), whereas Taxol may only trigger the BubR1-dependent pathway. While we see a reduction in BubR1 kinetochore localization after nocodazole treatment, the presence of substantial Mad2 at kinetochores in addition to reduced amounts of BubR1 is apparently sufficient for responding to loss of kinetochore-microtubule attachment. Although Bub1 was previously shown to be necessary for efficient localization of both Mad2 and BubR1 to kinetochores, our data suggest that Bub1 is more critical in the tension-sensitive BubR1 signaling pathway than in attachment sensing.

We show here that *Bub1*$^{\Delta 2\text{-}3/\Delta 2\text{-}3}$ MEFs rapidly develop a high frequency of aneuploidy that is likely explained by a weakened SAC response. Nocodazole-treated and Taxol-treated *Bub1*$^{\Delta 2\text{-}3/\Delta 2\text{-}3}$ MEFs have a reduced mitotic index relative to *wt* cells; yet, these assays are relatively crude and may not accurately measure weakened signaling capacity. A more sensitive test of SAC function comes when most chromosomes achieve bipolar attachment and tension, as the remaining signal from even a single unattached kinetochore must be sufficient to block anaphase onset until attachment and tension are achieved (41, 42). Under these conditions, insufficiency of SAC components may impair the SAC enough to allow anaphase onset, resulting in lagging chromosome(s). The high frequency of *Bub1*$^{\Delta 2\text{-}3/\Delta 2\text{-}3}$ cells with lagging chromosomes, coupled with the fact that only one or two such chromosomes are observed in most cells, suggests that chromosome missegregation in *Bub1*$^{\Delta 2\text{-}3/\Delta 2\text{-}3}$ cells is triggered by a defect in sensing minor, rather than catastrophic, mitotic aberrations. Bub1 has also been reported to play a role in chromosome congression and regulation of sister chromatid cohesion (15, 16, 19, 20). We observed an increase in chromosome congression errors in *Bub1*$^{\Delta 2\text{-}3/\Delta 2\text{-}3}$ MEFs, suggesting that this mechanism may contribute to the mitotic errors in these cells. However, the percentage of cells with obvious congression errors was low relative to the percentage with lagging chromosomes, suggesting that congression errors are unlikely to account for the full extent of missegregation observed. Moreover, noncongressed chromosomes should invoke a SAC arrest under normal conditions. Therefore, we argue that the mitotic defects in *Bub1*$^{\Delta 2\text{-}3/\Delta 2\text{-}3}$ MEFs are a consequence of impairment in both chromosome congression and SAC signaling.

A large body of evidence indicates that cellular senescence suppresses cellular proliferation in response to DNA damage and/or oncogene activation. Here, we show that *Bub1*$^{\Delta 2\text{-}3/\Delta 2\text{-}3}$ MEFs are significantly growth impaired and produce high levels of premature senescence. This effect was less severe in *Bub1*$^{\Delta 2\text{-}3/+}$ MEFs, which also displayed lower levels of aneuploidy. Thus, a major consequence of impaired Bub1 function and resulting chromosome segregation errors seems to be permanent cell cycle arrest. Increased senescence was also observed in *BubR1* hypomorph mice (12), which also display high rates of aneuploidy. Furthermore, aneuploid yeasts were recently shown to display impaired growth and metabolic changes accompanied by evidence of protein degradation and folding distress (43). Thus, it is possible that the increased metabolic demand of extra chromosomes taxes cellular machinery, causing a stress response that triggers senescence. Aneuploidy may also trigger stress responses by causing imbalances in signaling pathways.

Bub1 and tumor suppression

Aneuploidy has long been associated with cancers, raising the hypothesis that spindle checkpoint impairment may predispose to tumorigenesis (44–46). Indeed, the presence of *Bub1* mutations in human colon cancer cell lines (21) and murine lymphomas (22) fueled this hypothesis. Here, we show a causal relationship between impaired Bub1 function and predisposition to cancer. When analyzed in a background permissive to survival, impaired Bub1 function predisposed to a higher frequency and expanded spectrum of tumors relative to *wt* littermates. Tumors arose in aging mice, indicative of a low penetrance effect, consistent with the notion that noncatastrophic rates of aneuploidy can produce tumorigenic chromosomal imbalances. Mice heterozygous for a null mutation of other SAC genes also resulted in increased tumor incidence, either spontaneously [*Mad1* (36), *Mad2* (11), *Cenp-E* (37)] or after carcinogen treatment [*BubR1* (13) and *Bub3* (9)]. The recent work of Jeganathan and colleagues (38) showed an increasing tumor incidence with progressive loss of Bub1, reaching 55% in mice with ∼20% of endogenous Bub1 levels. The higher tumor incidence (76%) in our model correlates with the further reduction in Bub1 levels to <5% and the corresponding increase in mitotic abnormalities. A severe hypomorphic allele of *BubR1* caused only a modest increase in tumorigenesis; however, animals aged prematurely, potentially confounding the quantitative assessment of tumor incidence (12). *CENPE* haploinsufficiency, which also causes severe aneuploidy, was recently shown to have either protective or tumorigenic effects, depending on the genetic and environmental context (37). Thus, the influence of mitotic infidelity on tumor formation seems to be dependent on the cellular and genetic context and likely reflects a quantitative trait. The level of mitotic disruption may be critical for tumor formation, with high levels of chromosome missegregation incompatible with cell survival or activating tumor suppression pathways, such as senescence. Future study of the hypomorphic *Bub1*$^{\Delta 2\text{-}3}$ mutation in the context of an allelic series with other available *Bub1* mutations, in addition to alterations in senescence pathway factors, such as p53, should provide valuable insight into to the mechanistic relationship between mitotic aberration, chromosome instability, and cancer.

Supplementary Material

Refer to Web version on PubMed Central for supplementary material.

Acknowledgments

Grant support: NCI 2-R01-CA065773-11A1 (T. Van Dyke), NIH GM24364 (E.D. Salmon), and Leukemia and Lymphoma Society of America grant 5408-02 (D.O. Cowley).

We thank members of the Van Dyke and Salmon laboratories for helpful discussions and technical assistance, Virginia Godfrey, (Department of Pathology and Laboratory Medicine), for histopathology analysis, Larry Arnold and the UNC Flow Cytometry Core Facility for flow cytometry assistance, Randy Thresher and the UNC Animal Models Core for gene targeting, Steve Taylor (Faculty of Life Sciences, University of Manchester, Manchester, UK), for providing a Bub1 antibody, and Michael Chua and Wendy Salmon for providing expert assistance with confocal microscopy. We further acknowledge the use of Michael Hooker Microscopy Core Facility (UNC) equipment and resources funded by an anonymous private donor.

References

1. Lew DJ, Burke DJ. The spindle assembly and spindle position checkpoints. Annu Rev Genet. 2003; 37:251–82. [PubMed: 14616062]
2. Cleveland DW, Mao Y, Sullivan KF. Centromeres and kinetochores: from epigenetics to mitotic checkpoint signaling. Cell. 2003; 112:407–21. [PubMed: 12600307]
3. Musacchio A, Salmon ED. The spindle-assembly checkpoint in space and time. Nat Rev Mol Cell Biol. 2007; 8:379–93. [PubMed: 17426725]
4. Bernard P, Hardwick K, Javerzat JP. Fission yeast bub1 is a mitotic centromere protein essential for the spindle checkpoint and the preservation of correct ploidy through mitosis. J Cell Biol. 1998; 143:1775–87. [PubMed: 9864354]
5. Warren CD, Brady DM, Johnston RC, Hanna JS, Hardwick KG, Spencer FA. Distinct chromosome segregation roles for spindle checkpoint proteins. Mol Biol Cell. 2002; 13:3029–41. [PubMed: 12221113]
6. Vanoosthuyse V, Valsdottir R, Javerzat JP, Hardwick KG. Kinetochore targeting of fission yeast mad and bub proteins is essential for spindle checkpoint function but not for all chromosome segregation roles of bub1p. Mol Cell Biol. 2004; 24:9786–801. [PubMed: 15509783]
7. Dobles M, Liberal V, Scott ML, Benezra R, Sorger PK. Chromosome missegregation and apoptosis in mice lacking the mitotic checkpoint protein Mad2. Cell. 2000; 101:635–45. [PubMed: 10892650]
8. Kalitsis P, Earle E, Fowler KJ, Choo KH. Bub3 gene disruption in mice reveals essential mitotic spindle checkpoint function during early embryogenesis. Genes Dev. 2000; 14:2277–82. [PubMed: 10995385]
9. Babu JR, Jeganathan KB, Baker DJ, Wu X, Kang-Decker N, van Deursen JM. Rae1 is an essential mitotic checkpoint regulator that cooperates with Bub3 to prevent chromosome missegregation. J Cell Biol. 2003; 160:341–53. [PubMed: 12551952]
10. Wang Q, Liu T, Fang Y, et al. BUBR1 deficiency results in abnormal megakaryopoiesis. Blood. 2004; 103:1278–85. [PubMed: 14576056]
11. Michel LS, Liberal V, Chatterjee A, et al. MAD2 haploinsufficiency causes premature anaphase and chromosome instability in mammalian cells. Nature. 2001; 409:355–9. [PubMed: 11201745]
12. Baker DJ, Jeganathan KB, Cameron JD, et al. BubR1 insufficiency causes early onset of aging-associated phenotypes and infertility in mice. Nat Genet. 2004; 36:744–9. [PubMed: 15208629]
13. Dai W, Wang Q, Liu T, et al. Slippage of mitotic arrest and enhanced tumor development in mice with BubR1 haploinsufficiency. Cancer Res. 2004; 64:440–5. [PubMed: 14744753]
14. Fisk HA, Mattison CP, Winey M. Human Mps1 protein kinase is required for centrosome duplication and normal mitotic progression. Proc Natl Acad Sci U S A. 2003; 100:14875–80. [PubMed: 14657364]
15. Johnson VL, Scott MI, Holt SV, Hussein D, Taylor SS. Bub1 is required for kinetochore localization of BubR1, Cenp-E, Cenp-F and Mad2, and chromosome congression. J Cell Sci. 2004; 117:1577–89. [PubMed: 15020684]
16. Meraldi P, Sorger PK. A dual role for Bub1 in the spindle checkpoint and chromosome congression. EMBO J. 2005; 24:1621–33. [PubMed: 15933723]

17. Sharp-Baker H, Chen RH. Spindle checkpoint protein Bub1 is required for kinetochore localization of Mad1, Mad2, Bub3, and CENP-E, independently of its kinase activity. J Cell Biol. 2001; 153:1239–50. [PubMed: 11402067]
18. Chen RH. Phosphorylation and activation of Bub1 on unattached chromosomes facilitate the spindle checkpoint. EMBO J. 2004; 23:3113–21. [PubMed: 15241477]
19. Tang Z, Sun Y, Harley SE, Zou H, Yu H. Human Bub1 protects centromeric sister-chromatid cohesion through Shugoshin during mitosis. Proc Natl Acad Sci U S A. 2004; 101:18012–7. [PubMed: 15604152]
20. Kitajima TS, Hauf S, Ohsugi M, Yamamoto T, Watanabe Y. Human Bub1 defines the persistent cohesion site along the mitotic chromosome by affecting Shugoshin localization. Curr Biol. 2005; 15:353–9. [PubMed: 15723797]
21. Cahill DP, Lengauer C, Yu J, et al. Mutations of mitotic checkpoint genes in human cancers. Nature. 1998; 392:300–3. [PubMed: 9521327]
22. Lee H, Trainer AH, Friedman LS, et al. Mitotic checkpoint inactivation fosters transformation in cells lacking the breast cancer susceptibility gene, Brca2. Mol Cell. 1999; 4:1–10. [PubMed: 10445022]
23. Jaffrey RG, Pritchard SC, Clark C, et al. Genomic instability at the BUB1 locus in colorectal cancer, but not in non-small cell lung cancer. Cancer Res. 2000; 60:4349–52. [PubMed: 10969775]
24. Shigeishi H, Oue N, Kuniyasu H, et al. Expression of Bub1 gene correlates with tumor proliferating activity in human gastric carcinomas. Pathobiology. 2001; 69:24–9. [PubMed: 11641614]
25. Lee EC, Yu D, Martinez de Velasco J, et al. A highly efficient Escherichia coli-based chromosome engineering system adapted for recombinogenic targeting and subcloning of BAC DNA. Genomics. 2001; 73:56–65. [PubMed: 11352566]
26. Su H, Mills AA, Wang X, Bradley A. A targeted X-linked CMV-Cre line. Genesis. 2002; 32:187–8. [PubMed: 11857817]
27. Dimri GP, Lee X, Basile G, et al. A biomarker that identifies senescent human cells in culture and in aging skin *in vivo*. Proc Natl Acad Sci U S A. 1995; 92:9363–7. [PubMed: 7568133]
28. Cowley DO, Muse GW, Van Dyke T. A dominant interfering Bub1 mutant is insufficient to induce or alter thymic tumorigenesis *in vivo*, even in a sensitized genetic background. Mol Cell Biol. 2005; 25:7796–802. [PubMed: 16107724]
29. Friedman LS, Thistlethwaite FC, Patel KJ, et al. Thymic lymphomas in mice with a truncating mutation in Brca2. Cancer Res. 1998; 58:1338–43. [PubMed: 9537225]
30. Meijer HA, Thomas AA. Control of eukaryotic protein synthesis by upstream open reading frames in the 5′-untranslated region of an mRNA. Biochem J. 2002; 367:1–11. [PubMed: 12117416]
31. Taylor SS, Hussein D, Wang Y, Elderkin S, Morrow CJ. Kinetochore localisation and phosphorylation of the mitotic checkpoint components Bub1 and BubR1 are differentially regulated by spindle events in human cells. J Cell Sci. 2001; 114:4385–95. [PubMed: 11792804]
32. Taylor SS, Ha E, McKeon F. The human homologue of Bub3 is required for kinetochore localization of Bub1 and a Mad3/Bub1-related protein kinase. J Cell Biol. 1998; 142:1–11. [PubMed: 9660858]
33. Meraldi P, Honda R, Nigg EA. Aurora kinases link chromosome segregation and cell division to cancer susceptibility. Curr Opin Genet Dev. 2004; 14:29–36. [PubMed: 15108802]
34. Gjoerup OV, Wu J, Chandler-Militello D, et al. Surveillance mechanism linking Bub1 loss to the p53 pathway. Proc Natl Acad Sci U S A. 2007; 104:8334–9. [PubMed: 17488820]
35. Parrinello S, Samper E, Krtolica A, Goldstein J, Melov S, Campisi J. Oxygen sensitivity severely limits the replicative lifespan of murine fibroblasts. Nat Cell Biol. 2003; 5:741–7. [PubMed: 12855956]
36. Iwanaga Y, Chi YH, Miyazato A, et al. Heterozygous deletion of mitotic arrest-deficient protein 1 (MAD1) increases the incidence of tumors in mice. Cancer Res. 2007; 67:160–6. [PubMed: 17210695]
37. Weaver BA, Silk AD, Montagna C, Verdier-Pinard P, Cleveland DW. Aneuploidy acts both oncogenically and as a tumor suppressor. Cancer Cell. 2007; 11:25–36. [PubMed: 17189716]

38. Jeganathan K, Malureanu L, Baker DJ, Abraham SC, van Deursen JM. Bub1 mediates cell death in response to chromosome missegregation and acts to suppress spontaneous tumorigenesis. J Cell Biol. 2007; 179:255–67. [PubMed: 17938250]
39. Perera D, Tilston V, Hopwood JA, Barchi M, Boot-Handford RP, Taylor SS. Bub1 maintains centromeric cohesion by activation of the spindle checkpoint. Dev Cell. 2007; 13:566–79. [PubMed: 17925231]
40. Skoufias DA, Andreassen PR, Lacroix FB, Wilson L, Margolis RL. Mammalian mad2 and bub1/bubR1 recognize distinct spindle-attachment and kinetochore-tension checkpoints. Proc Natl Acad Sci U S A. 2001; 98:4492–7. [PubMed: 11274370]
41. Rieder CL, Cole RW, Khodjakov A, Sluder G. The checkpoint delaying anaphase in response to chromosome monoorientation is mediated by an inhibitory signal produced by unattached kinetochores. J Cell Biol. 1995; 130:941–8. [PubMed: 7642709]
42. Rieder CL, Schultz A, Cole R, Sluder G. Anaphase onset in vertebrate somatic cells is controlled by a checkpoint that monitors sister kinetochore attachment to the spindle. J Cell Biol. 1994; 127:1301–10. [PubMed: 7962091]
43. Torres EM, Sokolsky T, Tucker CM, et al. Effects of aneuploidy on cellular physiology and cell division in haploid yeast. Science. 2007; 317:916–24. [PubMed: 17702937]
44. Kops GJ, Weaver BA, Cleveland DW. On the road to cancer: aneuploidy and the mitotic checkpoint. Nat Rev Cancer. 2005; 5:773–85. [PubMed: 16195750]
45. Rajagopalan H, Lengauer C. Aneuploidy and cancer. Nature. 2004; 432:338–41. [PubMed: 15549096]
46. Bharadwaj R, Yu H. The spindle checkpoint, aneuploidy, and cancer. Oncogene. 2004; 23:2016–27. [PubMed: 15021889]

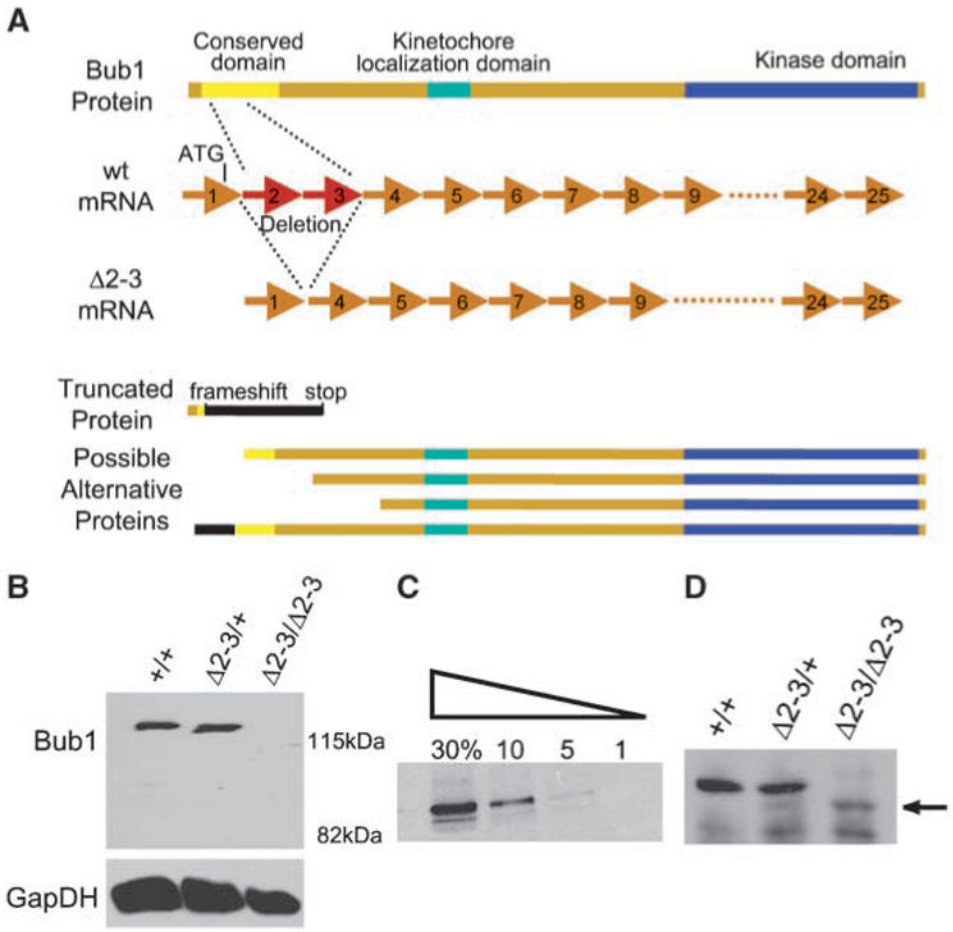

Figure 1.

Bub1 gene disruption. *A*, the $Bub^{\Delta 2\text{-}3}$ allele removes a portion of the NH_2 terminal conserved domain. *Top*, schematic of Bub1 protein domains and corresponding exons; *bottom*, possible protein products produced from the $Bub^{\Delta 2\text{-}3}$ allele. *B*, Western blot analysis of endogenous Bub1 protein in MEFs of indicated genotypes. No protein is detected from $Bub1^{\Delta 2\text{-}3/\Delta 2\text{-}3}$ cells. GapDH was used as a loading control. *C*, titration of lysate from $Bub1^{+/+}$ MEFs indicating that the Bub1 antibody detects 5% of endogenous levels. *D*, immunoprecipitation–Western blot. Arrow indicates a novel polypeptide detected in lysates from cells harboring the $Bub1^{\Delta 2\text{-}3}$ allele.

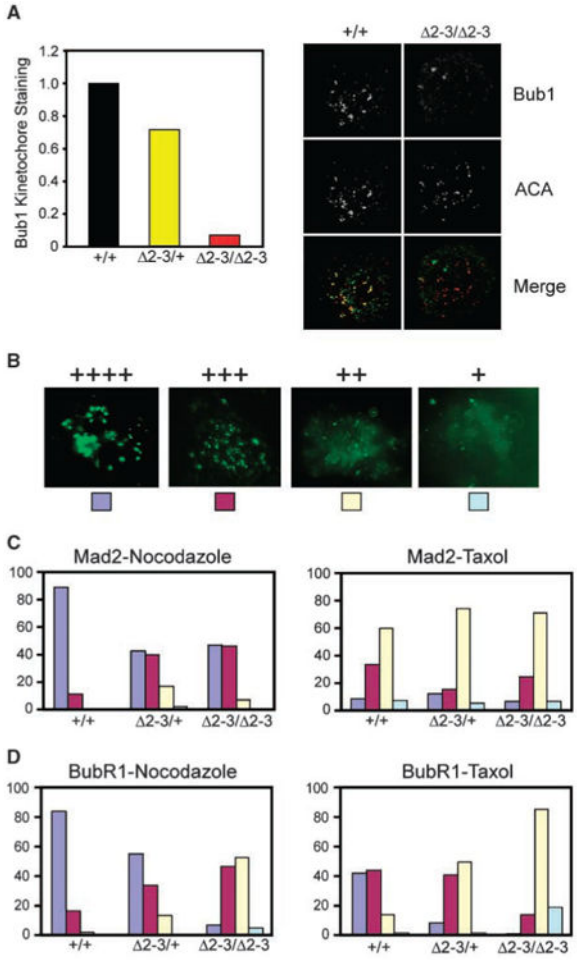

Figure 2.

Bub1 and BubR1 are reduced at kinetochores in *Bub1*$^{\Delta 2\text{-}3/\Delta 2\text{-}3}$ MEFs. *A*, *left*, quantitation of Bub1 levels at kinetochores normalized to ACA (centromere marker); *right*, representative Bub1, ACA, and merged images from *wt* and *Bub1* mutant MEFs. *B*, representative images illustrating staining level classifications used in quantitations for C-D. C, Mad2 kinetochore localization after treatment with nocodazole (*left*) and Taxol (*right*). *Bars*, percentage of cells of each class depicted in *B*. *D*, BubR1 kinetochore localization after treatment with nocodazole (*left*) and Taxol (*right*). $n = 50$ cells each from three individual experiments for *C* and *D*.

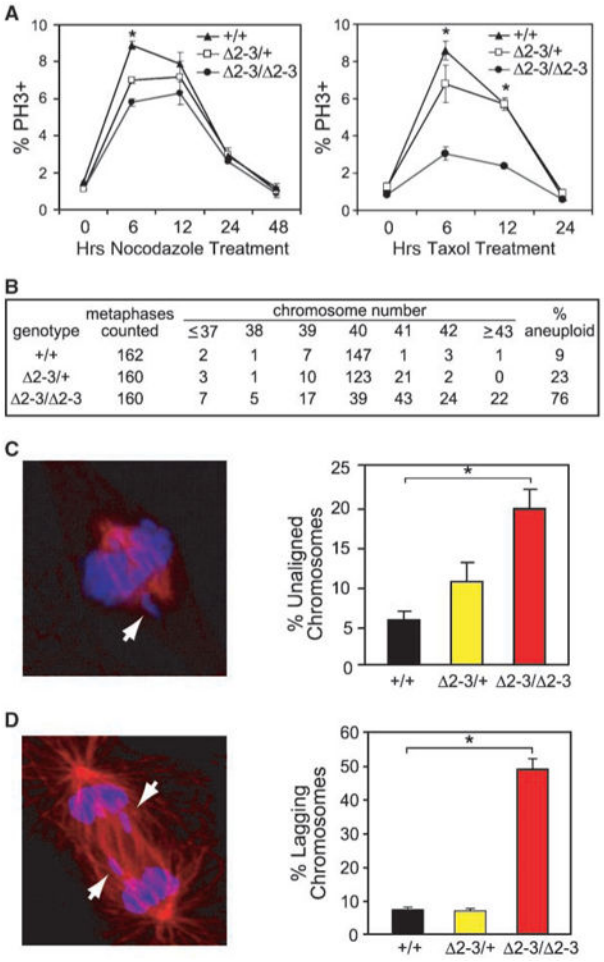

genotype	metaphases counted	chromosome number ≤37	38	39	40	41	42	≥43	% aneuploid
+/+	162	2	1	7	147	1	3	1	9
Δ2-3/+	160	3	1	10	123	21	2	0	23
Δ2-3/Δ2-3	160	7	5	17	39	43	24	22	76

Figure 3.

Bub1$^{\Delta 2\text{-}3/\Delta 2\text{-}3}$ MEFs have reduced spindle checkpoint activity and increased mitotic abnormalities. *A*, accumulation of mitotic (phosphorylated histone H3-positive) cells after nocodazole treatment (*left*) and Taxol treatment (*right*). *B*, incidence of aneuploid cells in P5 MEFs. *C*, quantitation of uncongressed chromsomes after 3 h of MG132 treatment with representative image of a metaphase nucleus with an uncongressed chromosome. *D*, quantitation of anaphase lagging chromosomes with representative image. Graphs in *A*, *C*, and *D* represent mean and SE of three independent experiments for each genotype with at least 10,000 cells analyzed per genotype per experiment in *A* and at least 50 cells per genotype per experiment for *C* and *D*. *, $P < 0.05$.

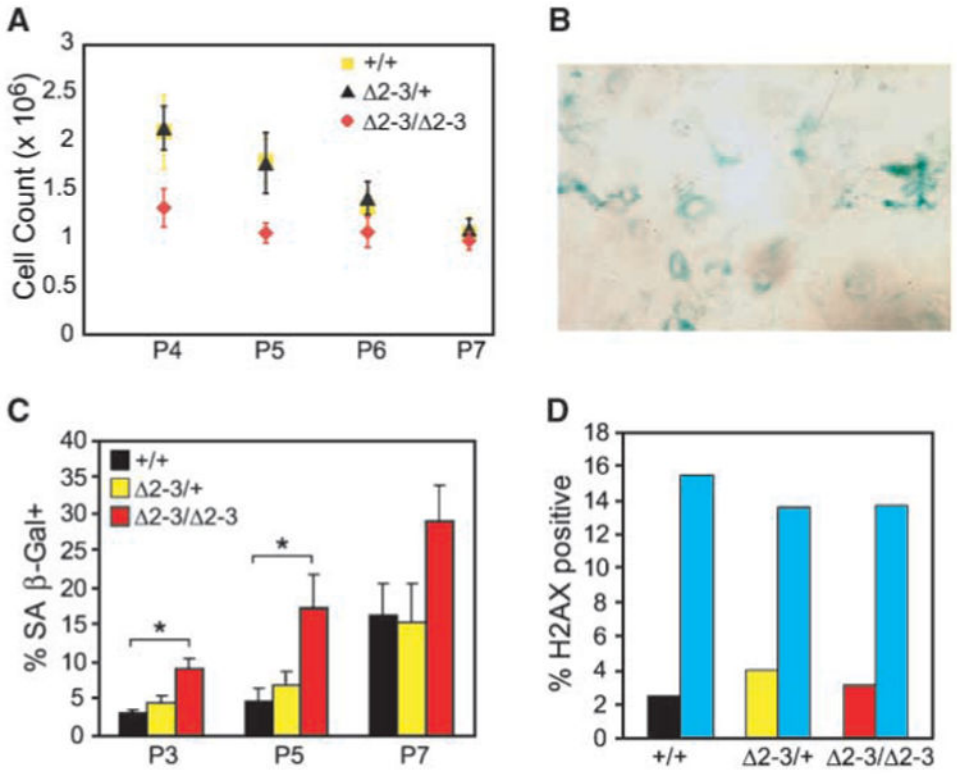

Figure 4.

Bub1$^{\Delta 2\text{-}3/\Delta 2\text{-}3}$ MEFcultures have reduced growth and increased senescence. *A*, total cell numbers accumulated at indicated passages. Cells (500,000) were plated at each passage (lower markers) and total cells counted upon passage 2 d later (top markers). *B*, representative acidic β-galactosidase staining (*blue*) of a *Bub1*$^{\Delta 2\text{-}3/\Delta 2\text{-}3}$ culture. *C*, senescent cells as a percentage of total cells at passages 3, 5, and 7. $n = 3$ independent experiments per genotype. *D*, *Bub1*$^{\Delta 2\text{-}3/\Delta 2\text{-}3}$ MEFs do not show increased DNA damage. Percentage of cells positive for phosphorylated H2AX immunostaining. Teal bars indicate duplicate control samples treated with doxorubicin to induce DNA damage. *, $P < 0.05$. *Bars*, SE.

A

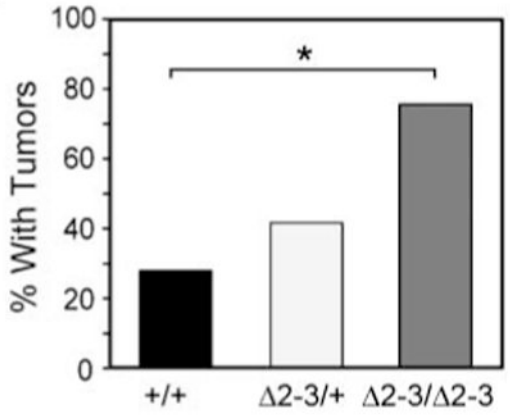

B

	+/+	Δ2-3/+	Δ2-3/Δ2-3
N	21	26	25
# w/ tumors	6	11	20
tumor type			
Liver	3	7	13
Lung		1	3
Ovary	1	1	1
Lymphoma	2	1	1
Liver&Lung			1
Brain		1	

Figure 5.

Tumor incidence and spectrum is increased with Bub1 mutation. *A*, tumor incidence in *Bub1*$^{\Delta 2\text{-}3/\Delta 2\text{-}3}$ mice and controls. *B*, tumor spectrum.

Table 1

Viability of Bub1 mutant mice

Genotype	Background	Live births	E18.5	E14.5
Bub1$^{\Delta 2\text{-}3/+}$ × *Bub1*$^{\Delta 2\text{-}3/+}$				
+/+	B6	68	26	17
Δ*2-3*/+		109	39	34
Δ*2-3*/Δ*2-3*		18* (2)†	22	18
+/+	FVB	33		
Δ*2-3*/+		76		
Δ*2-3*/Δ*2-3*		35		
+/+	B6/129	162		15
Δ*2-3*/+		353		23
Δ*2-3*/Δ*2-3*		96		14
Bub1$^{\Delta 2\text{-}3/+}$ × *Bub1*$^{gt8/+}$				
+/+	B6/129	40		10
Δ*2-3*/+		30		27
gt8/+		21		10
Δ*2-3*/*gt8*		0		0

*$P < 0.005$.

†Two mice survived to weaning at 21 d.